ISSN: 2447-3359

REVISTA DE GEOCIÊNCIAS DO NORDESTE

Northeast Geosciences Journal

v. 11, nº 1 (2025)

https://doi.org/10.21680/2447-3359.2025v11n1ID35122

Slope stability analysis using a probabilistic approach

Análise de estabilidade de taludes usando uma abordagem probabilística

Matheus Veras Neves[1]; Thâmara Ingrid Costa Garcês[2]; George Fernandes Azevedo[3]; Felipe Alexander Vargas Bazán[4]; Paulo César de Oliveira Queiroz[5]; Ronnan Wembles Martins Barreira[6]; Luanne de Fátima Pereira Batalha[7]

[1] Federal University of Maranhão, Department of Civil Engineering, São Luís/MA, Brazil. Email: matheus.vneves@gmail.com
ORCID: https://orcid.org/0000-0003-4246-2089

[2] Federal University of Maranhão, Department of Civil Engineering, São Luís/MA, Brazil. Email: thamaragarces@gmail.com
ORCID: https://orcid.org/0009-0007-8404-8456

[3] Federal University of Maranhão, Department of Civil Engineering, São Luís/MA, Brazil. Email: gf.azevedo@ufma.br
ORCID: https://orcid.org/0000-0002-2207-7282

[4] Federal University of Maranhão, Department of Civil Engineering, São Luís/MA, Brazil. Email: felipe.vargas@ufma.br
ORCID: https://orcid.org/0000-0001-6799-0799

[5] Federal University of Maranhão, Department of Civil Engineering, São Luís/MA, Brazil. Email: pco.queiroz@ufma.br
ORCID: https://orcid.org/0000-0002-8905-1757

[6] Federal University of Maranhão, Department of Civil Engineering, São Luís/MA, Brazil. Email: ronnan-wmb@hotmail.com
ORCID: https://orcid.org/0000-0003-1176-5191

[7] Federal University of Maranhão, Department of Civil Engineering, São Luís/MA, Brazil. Email: luannebatalha@gmail.com
ORCID: https://orcid.org/0009-0000-7955-891X

Abstract: This paper presents a study that uses computational implementations of the FOSM and Monte Carlo methods. These methods aim to determine the probability of slope rupture in areas prone to shallow landslides. The study focuses on the Vila Rabelo region situated in the administrative zone of Sobradinho II, Federal District. The computational approach involves two distinct programming tools: MATLAB for the FOSM method, and FORTRAN for the Monte Carlo simulation method. The analysis reveals that the Monte Carlo method tends to yield higher maximum rupture probability values compared to the FOSM method, particularly in steep terrain. A convergence analysis for the Monte Carlo method was undertaken to illustrate how the appropriate number of simulations is determined. Furthermore, findings indicate spatial proximity and occasionally higher values in the spatial distribution of rupture probabilities obtained from the Monte Carlo method compared to the FOSM method. The variations in rupture probability values achieved through probabilistic methods result from the distribution configurations of the cohesion variable, which is one of the input data.
Keywords: Landslides; Probabilistic approach; Slope stability.

Resumo: Este artigo apresenta um estudo que utiliza implementações computacionais dos métodos FOSM e Monte Carlo. Estes métodos visam determinar a probabilidade de ruptura de encostas em áreas suscetíveis a deslizamentos rasos. O estudo concentra-se na região da Vila Rabelo, situada na zona administrativa de Sobradinho II, Distrito Federal. A abordagem computacional emprega duas ferramentas de programação distintas: o MATLAB para o método FOSM, e o FORTRAN para o método de simulação de Monte Carlo. A análise revela que o método Monte Carlo tende a produzir valores de probabilidade de ruptura mais elevados em comparação com o método FOSM, especialmente em terrenos íngremes. Foi realizada uma análise de convergência para o método de Monte Carlo, a fim de ilustrar como é determinado o número de simulações adequado. Além disso, os resultados indicam proximidade espacial e ocasionalmente valores mais altos na distribuição espacial de probabilidades de ruptura obtidas a partir do método Monte Carlo em comparação com o método FOSM. As variações nos valores de probabilidade de ruptura alcançados por meio de métodos probabilísticos decorrem das configurações de distribuição da variável coesão, que é um dos dados de entrada.

Palavras-chave: Movimentos de massa; Abordagem probabilística; Estabilidade de taludes.

Received: 17/01/2024; Accepted: 06/09/2024; Published: 28/01/2025.

1. Introduction

Landslides, along with floods, are disasters with a high incidence rate worldwide. They result in social and economic impacts on societies, particularly in densely populated urban areas and rugged terrains. Estimates indicate that the number of landslides recorded globally exceeds that of other natural hazards, including earthquakes, hurricanes, and volcanoes (CHEN; LEE, 2004).

In Brazil, research on landslides was prompted by the work of Guidicini e Nieble (1984), which offered a systematic classification of these events, their causes, and agents, along with methods for calculating slope stability. According to Furlan, Lacruz e Susen (2011), landslides' disasters in Brazil result from a combination of adverse events and physical and socioeconomic vulnerabilities. This highlights the need of spatially identifying susceptible areas for event occurrence, defining hazards, and identifying risk-enhancing attributes.

Due to the various factors involved in landslide processes and the numerous pieces of information that need to be considered in risk and susceptibility analysis, Geographic Information Systems (GIS) have been widely used in conjunction with physical models (VENANCIO *et al.*, 2013). The one-dimensional infinite slope model is one of the most frequently used approaches for analyzing slope stability (COLLINS; ZNIDARCIC, 1998; CHO; LEE, 2002; FRATTINI *et al.*, 2004). The SHALSTAB model was proposed and validated by Montgomery and Dietrich (1994) and this is another highly recognized technique. This model assesses soil saturation as a function of rainfall infiltration through a topographic index, highlighting that surface topography serves as a primary indicator for predicting shallow landslide occurrences. As a result, this model holds significant value by effectively identifying highly susceptible areas for landslides under rainfall influence.

The utilization of probabilistic techniques, such as the First Order Second Moment (FOSM), Point Estimates, and Monte Carlo methods, in reliability analyses, enables a more comprehensive handling of uncertainties in geotechnical design processes. While the application of reliability methods does not ensure the prevention of failures, their systematic and meticulous implementation allows engineers to discern which uncontrollable factors will significantly impact such failures (MONTOYA; ASSIS, 2011).

For instance, Azevedo, Carvajal e Souza (2018) studied a region within the Federal District, performing an analysis of susceptibility to landslide occurrences. The use of a probabilistic approach enabled the incorporation of parameter variability within the slope stability evaluation model, yielding hazard outcomes in terms of failure probabilities. Martini *et al.* (2006) employed GIS and multicriteria decision techniques to assess susceptibility to erosive processes and landslides in Santa Catarina, specifically around the Quebra-Queixo dam. Their study yielded a thematic map, integrating parameters such as terrain relief, soil composition, and land cover, thereby illustrating the spatial distribution of susceptibility classes to the aforementioned processes in the vicinity of the reservoir dam.

This article addresses the computational implementation of methods capable of determining the probability of slope failure in areas susceptible to shallow landslides, specifically the First Order Second Moment (FOSM) method and the Monte Carlo simulation method. Besides facilitating various applications within geotechnical studies concerning slope stability, such as evaluating reliability and the uncertainty associated with rock mechanics and natural disasters, these methods also enable the derivation of indices for susceptibility assessment.

2. Definition and Contextualization of the Study Area

Vila Rabelo, the study area evaluated in this research, is situated in the administrative region of Sobradinho II, Federal District, Brazil. According to data from the District Household Sample Survey – PDAD 2018 (CODEPLAN, 2019), the urban population of Sobradinho II was 85.574 inhabitants, and its area was approximately 285 km². The region experienced rapid population growth in the 1990s due to the Low-Income Population Settlement Program.

This area provides shelter for families living in vulnerable conditions and is situated on irregular land amidst 23 condominiums. A survey conducted in 2012 by the Civil Defense of the Federal District employed mapping to identify multiple risk zones within the Vila Rabelo region, recognizing 421 residences susceptible to various degrees of instability.

Vila Rabelo has a history of territorial organization issues. Recurrent landslides occur due to the placement of the population's residences in the region. The Civil Defense study identified 209 sites at risk of landslides in both Vila Rabelo I and Vila Rabelo II. Figure 1 provides a precise depiction of the area delineated for this research.

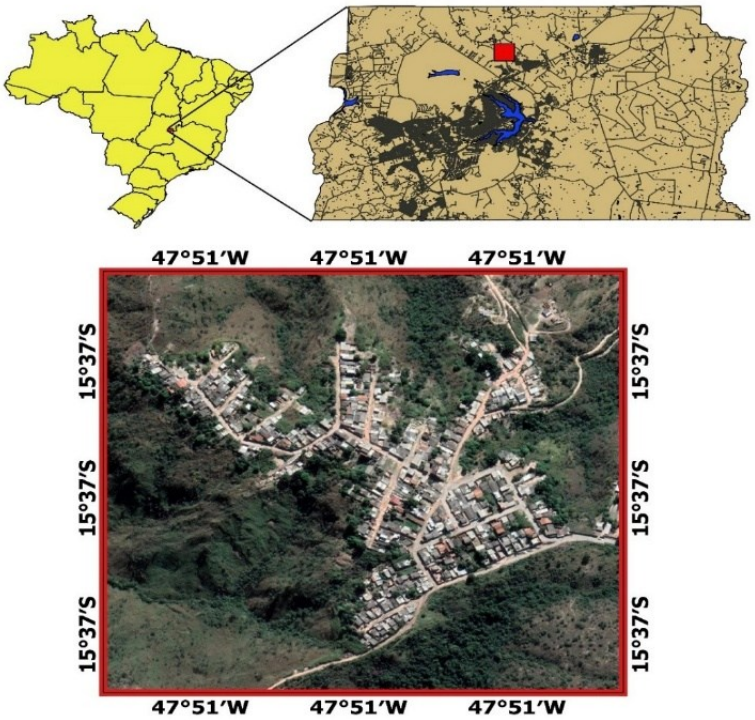

Figure 1 – Study area.
Source: Authors (2024).

3. Methodology

The methodology proposed for this research involved the computational implementation of methods capable of determining the probability of failure in areas prone to shallow landslides, coupled with a stability model. Specifically, the methods employed were the First Order Second Moment (FOSM) method and the Monte Carlo simulation method.

The computational implementation utilized two distinct programming tools: MATLAB (Matrix Laboratory) and FORTRAN (Formula Translator). FORTRAN was chosen for the Monte Carlo method due to its complexity and high computational demand, necessitating a medium-level performance language for efficient data processing and handling a substantial number of simulations. For the simpler FOSM method, MATLAB was selected as it offers user-friendly software and aligns with the method's simplicity.

The computational platform known as Spring 5.4.3 (CÂMARA *et al.*, 1996), built upon Geographic Information Systems (GIS), was utilized to manage the spatial information of the covered region. This involved establishing a dedicated database and project for the research. The QGIS software was employed to produce the final map presentations.

The spatial input data comprise topography and soil maps. The topographic map is obtained from the Brasilia State Company TERRACAP, with a matrix format and a spatial resolution of 5 m. This layer formed the foundation for creating the terrain slope matrix (Figure 2).

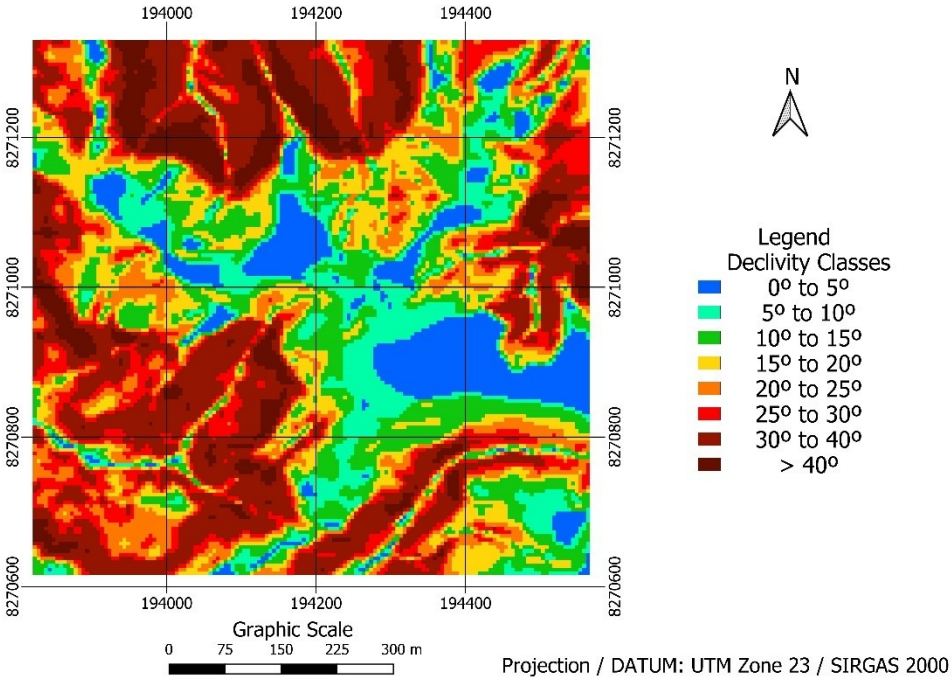

Figure 2 – Terrain slope map.
Source: Authors (2024).

The study area was discretized into pixels, matching the same spatial resolution as the topographic map, resulting in a matrix composed of 152 columns and 147 rows.

The soil map used is an updated version of the digital pedological map of the Federal District, as proposed by Reatto *et al.* (2004). The entire study area falls within the domain of Cambisol.

Various methods are available to assess slope stability. In situations where the potential failure plane is nearly parallel to the ground surface, the infinite slope method can be applied (CORDOBA; MERGILI; ARISTIZÁBAL, 2020). In such cases, the expression for the safety factor is given by Equation 1:

$$FS = \frac{c' + \gamma.h.cos^2\theta.tan\varphi'}{\gamma.h.sen\theta.cos\theta} \quad (1)$$

Where c' is the effective soil cohesion, γ is the specific weight of the soil, h is the thickness of the soil layer, θ is the inclination (slope) of the soil, and φ' is the effective friction angle of the soil.

The average values for the model parameters related to the Cambisol pedological class are derived from the study by Azevedo, Carvajal e Souza (2018) and are drawn from scientific literature on geotechnical soil characterization within the Federal District. The mean model parameters are presented in Table 1.

Table 1 – Strength parameters and specific weight of the soil..

Soil	**Soil parameters**		
	c'	φ'	γ
	kPa	°	kN/m³
Haplic Cambisol	5	25	15

Source: Authors (2024).

A predictive empirical model proposed by Catani, Segoni e Falorni (2010) was employed to depict the spatial variability of soil thickness in the study area. This model is described by Equation 2:

$$h_i = h_{max}.\left[1 - \frac{tan\theta_i - tan\theta_{min}}{tan\theta_{max} - tan\theta_{min}}.\left(1 - \frac{h_{min}}{h_{max}}\right)\right] \quad (2)$$

The equation above establishes a correlation between the soil thickness at a given pixel and corresponding representative slope angle of the cell. In this equation, h_i represents the soil thickness in pixel i; h_{max} and h_{min} denote the maximum and minimum measured soil thickness values within the area, respectively. The value of θ_i indicates the local slope at a pixel i, whereas θ_{max} and θ_{min} indicate the maximum and minimum slope (or inclination) values observed at the test site. For the analyses, the scenario was adopted with h_{min} = 0.7 m and h_{max} = 2 m. The utilization of this model is justified by the study area's uniform soil type. Thus, incorporating soil thickness variability based on the relief criterion becomes feasible.

It's crucial to note that the land slope directly impacts water accumulation. On steeper slopes, there's a tendency for shallower soils with limited water infiltration and percolation. Rain can wash away particles. Conversely, flatter areas are prone to water buildup, characterized by percolation and slower runoff.

3.1 Probabilistic methods

In the probabilistic analysis, two random variables were taken into consideration: cohesion and friction angle. The remaining parameters in Equation 1 were treated as deterministic: specific weight, soil thickness, and slope. According to Tonus (2009), cohesion was modeled by a lognormal probability distribution with a coefficient of variation of 40%. Meanwhile, the friction angle was modeled using a normal probability distribution with a coefficient of variation of 10%.

In the probabilistic approach, it is necessary to establish a performance function, also known as a limit state function. This function relies on the random variables pertinent to the issue. In this instance, the performance function is derived from the safety factor of the infinite slope method:

$$g = g(c', \varphi') = FS(c', \varphi') - 1 \quad (3)$$

In this equation, the interdependence of random variables is clearly highlighted. Negative values of the performance function correspond to rupture, while positive values indicate safety. Hence, the probability of rupture, denoted as P_r, is calculated by determining the probability that the performance function yields negative values, or mathematically, P_r = P[$\{g \leq 0\}$].

3.2 FOSM Method

In the FOSM method, the calculation methodology involves employing the first-order terms of a Taylor series expansion of the performance function centered around the mean value of each random variable.

In the specific problem at hand, wherein the random variables encompass cohesion and friction angle, Equation 4 offers a primary approximation for the mean value, or expected value, of the safety factor:

$$E[FS] = FS\left(\mu_{c\prime}, \mu_{\varphi\prime}\right) \quad (4)$$

Here, c' and φ' denote the mean values of cohesion and friction angle, respectively. Thus, the second term in Equation 4 represents the evaluation of the safety factor using the mean values of the random variables.

On the other hand, assuming statistical independence among the random variables of the problem, Equation 5 offers a first-order approximation for the variance of the safety factor.

$$Var(FS) = Var(c').\left(\frac{\partial FS}{\partial c\prime}\right)^2 + Var(\varphi').\left(\frac{\partial FS}{\partial \varphi\prime}\right)^2 \quad (5)$$

In this equation, *Var(c')* and *Var(φ')* represent the variances of cohesion and friction angle, respectively. Additionally, $\partial FS/\partial c'$ and $\partial FS/\partial \varphi'$ denote the partial derivatives of the factor of safety concerning cohesion and friction angle,

respectively. These derivatives are evaluated using the mean values of the respective random variables. Notably, in this study, the partial derivatives were analytically determined.

Within the framework of the FOSM method, given the performance function delineated in Equation 6, the reliability index, as outlined by Cornell (1969), is derived as follows:

$$\beta = \frac{E[FS]-1}{\sqrt{Var(FS)}} \tag{6}$$

Utilizing the reliability index defined in Equation 6, it becomes feasible to deduce the subsequent first-order approximation for the probability of failure:

$$P_r = \varphi(-\beta) \tag{7}$$

Where $\varphi(\cdot)$ represents the cumulative distribution function of the standard normal distribution.

For implementing the FOSM method computationally, a code was developed utilizing the MATLAB software. This code processed input data encompassing slope inclination, soil thickness, and soil specific weight, along with the mean values of cohesion and friction angle.

By employing Equations 4 to 7, the reliability index and probability of failure were computed for each pixel. Consequently, this process yielded a numerical matrix containing the failure probability values across the entire study area.

3.2 Monte Carlo Simulation Method

Monte Carlo simulation involves the utilization of random numbers. This method encompasses numerically simulating an extensive array of scenarios, ideally encapsulating all conceivable combinations of the problem's random variables. Such numerical simulations are executed, grounded in the probability distributions of the said variables.

In the context of the examined problem, every simulation involves generating cohesion and friction angle samples (which are independent random variables). Subsequently, the value of the performance function is computed through Equation 8 to ascertain whether the simulated scenario aligns with a failure condition ($g \leq 0$, or $FS \leq 1$) or not ($g > 0$, or $FS > 1$). This iterative process is reiterated numerous times. Consequently, a straightforward estimate of the probability of failure can be obtained as follows:

$$P_r = \frac{N_r}{N} \tag{8}$$

In this equation, N_r signifies the count of simulations where failure occurred (i.e., the simulations with $g \leq 0$), and N stands for the overall number of simulations. As per Wyllie e Mah (2004), it is imperative that N be greater than 100.

The Monte Carlo simulation method is fundamentally founded on the generation of random numbers, uniformly distributed within the range of 0 and 1. In the context of this study, this process was executed through what is known as a linear congruential generator. This algorithm's behavior is governed by a collection of constants that impart its distinctive traits. In this regard, values suggested by Beck (2019) have been employed. Furthermore, this generator requires the user to provide an initial "seed" value - an integer used to start the simulation process.

Samples of the random variables pertaining to the problem were generated from uniformly distributed random numbers, following a method elucidated in the literature (e.g., NOWAK; COLLINS, 2013; BECK, 2019). This approach relies on the established probability distributions of the random variables.

To achieve the computational implementation of the Monte Carlo method, a code was developed using the Fortran language. Within this code, inputs encompass the slope inclination, soil thickness, soil specific weight, and the mean values of cohesion and friction angle. Moreover, the code necessitates input values for the count of Monte Carlo simulations and the "seed" of the random number generator.

The executed procedure computes the probability of failure for each cell using Equation 8, culminating in the generation of a matrix that encapsulates numerical values representing the probabilities of failure across the entire study area.

Hence, within the study area, the Monte Carlo method was employed using varying simulation quantities: $1x10^4$ (ten thousand), $5x10^4$ (fifty thousand), $1x10^5$ (one hundred thousand), $1x10^6$ (one million), and $1x10^7$ (ten million). This process yielded matrices that encompass the probability of failure for each respective case. Subsequently, an assessment of the probability of failure's fluctuation concerning the number of simulations was undertaken at distinct pixels, coinciding with

grid points that possess the highest and lowest slopes. Through this scrutiny, it became feasible to ascertain how the probability of failure behaves across diverse simulation quantities in the Monte Carlo method.

4. Results and discussion

Utilizing the outcome matrices produced by the computational implementations of the FOSM and Monte Carlo methods, it became feasible to derive probability of failure maps for the study area. To achieve this, the class slicing procedure within the Spring software was employed. The slicing operation consisted of generating a thematic image based on the rectangular grid of probability of failure. The slicing operation considered the numerical matrices obtained from the analyses as input data. Then, the value of each cell in the study area was associated with a range of failure probability values, which would be the corresponding thematic class. Initially, thematic categories related to probabilities of failure were created separately to represent the results of the FOSM and Monte Carlo methods. From this, the definition of the slice intervals was carried out based on the variation of the resulting grid values in each simulation. These resultant maps are visually represented in Figures 3 to 8.

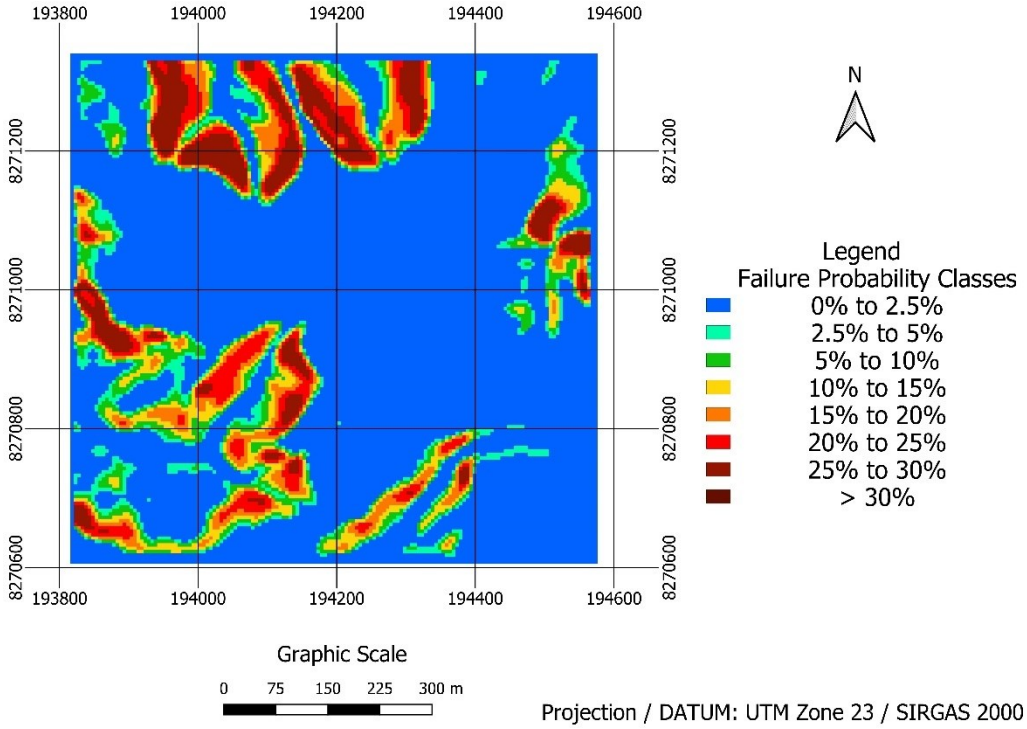

Figure 3 – Probability of Failure Map for the FOSM method.
Source: Authors (2024).

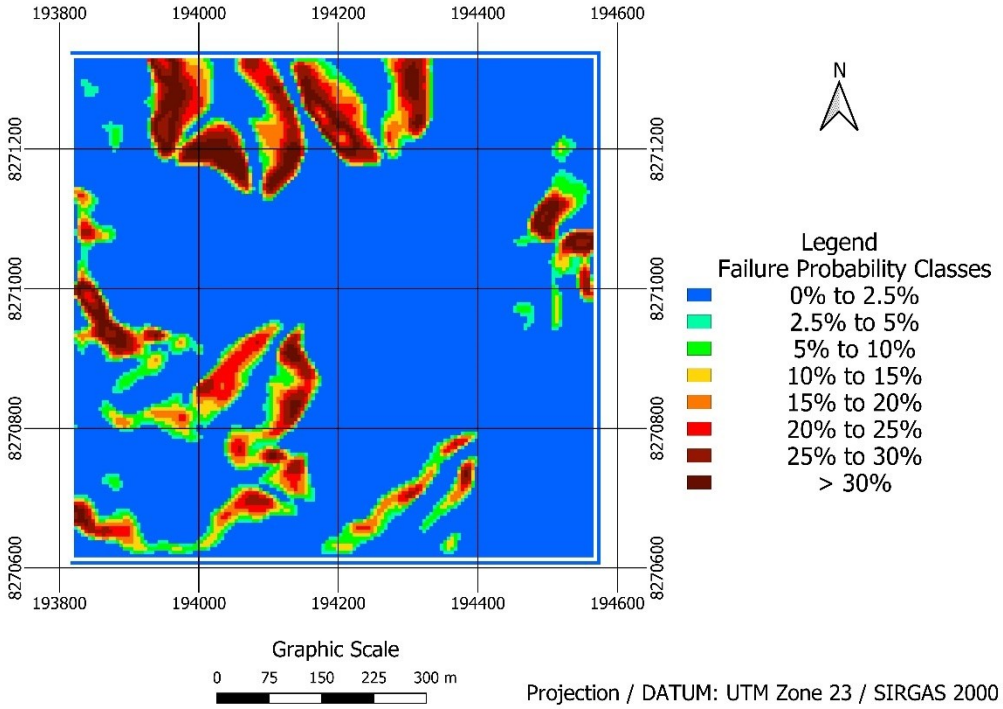

Figure 4 – Monte Carlo Probability of Failure Map (1x10^4 simulations).
Source: Authors (2024).

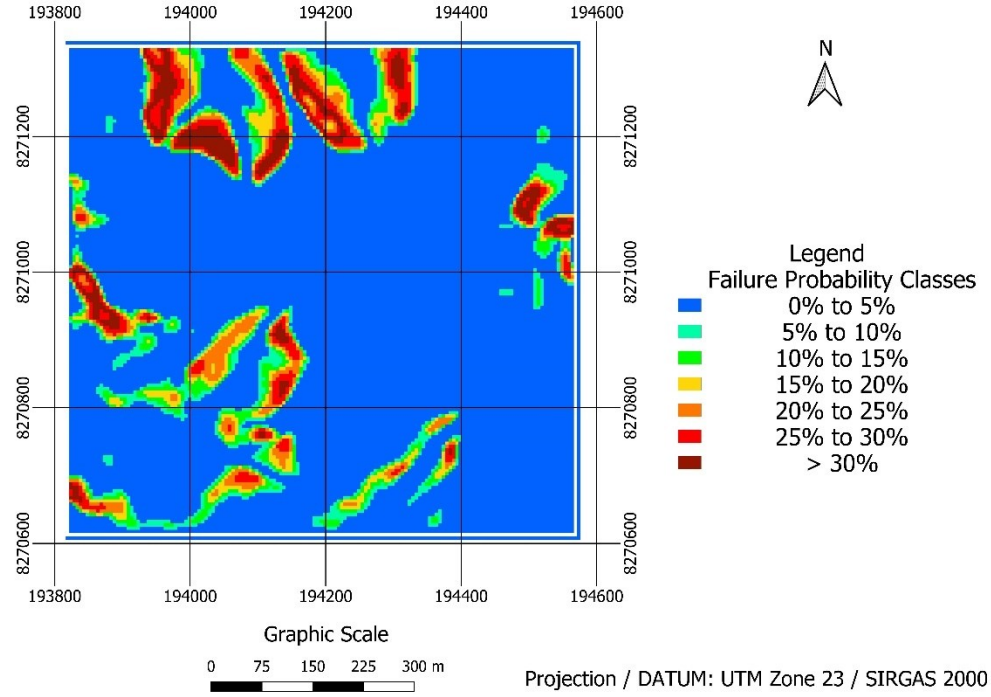

Figure 5 – Monte Carlo Probability of Failure Map (5x10^4 simulations).
Source: Authors (2024).

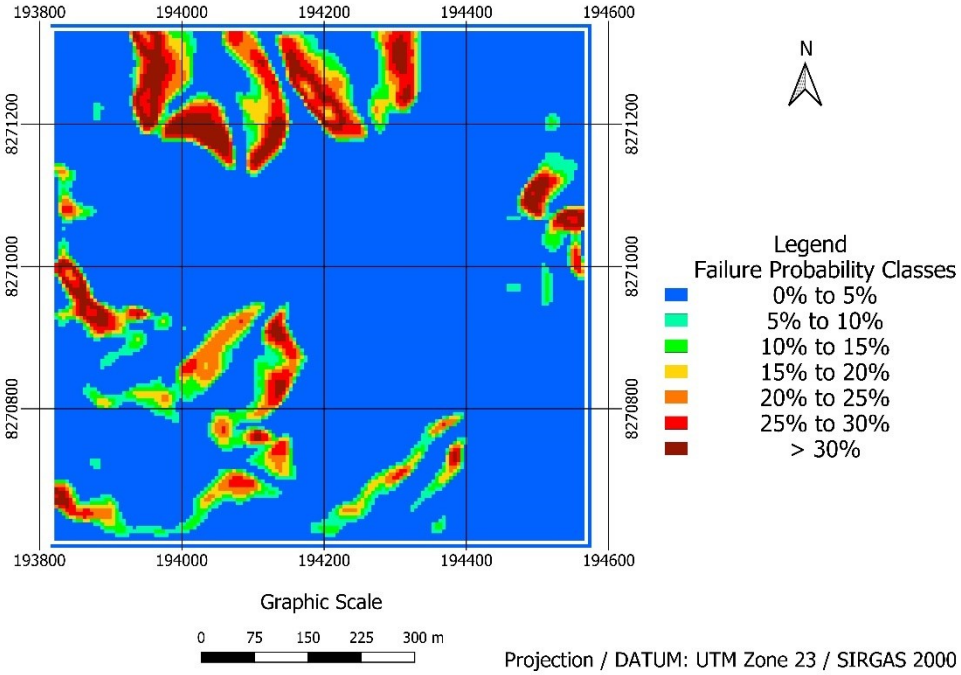

Figure 6 – Monte Carlo Probability of Failure Map (1x10^5 simulations).
Source: Authors (2024).

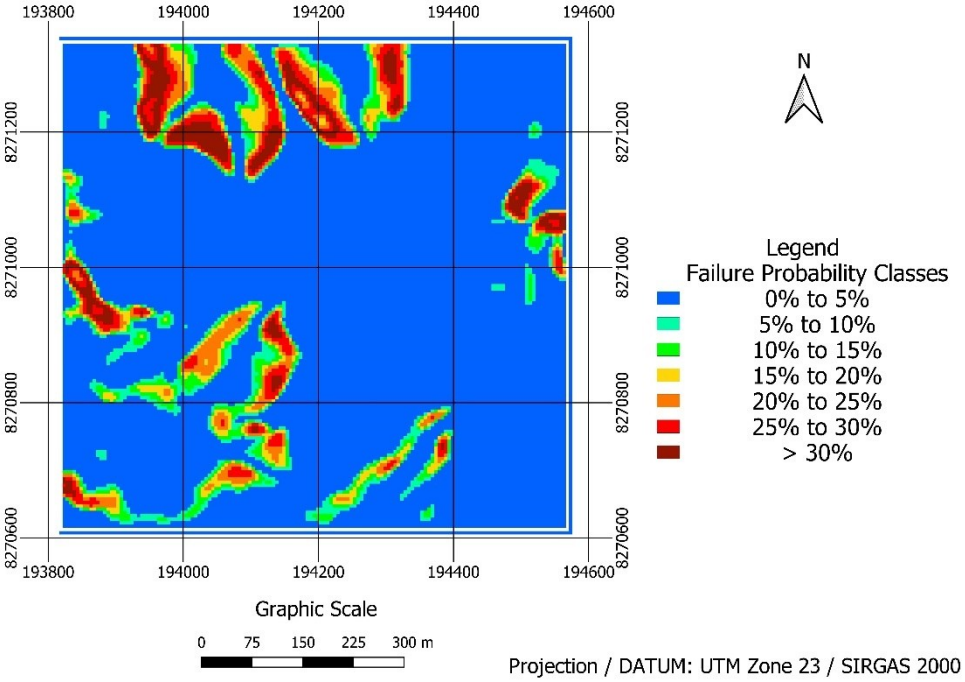

Figure 7 – Monte Carlo Probability of Failure Map (1x10^6 simulations).
Source: Authors (2024).

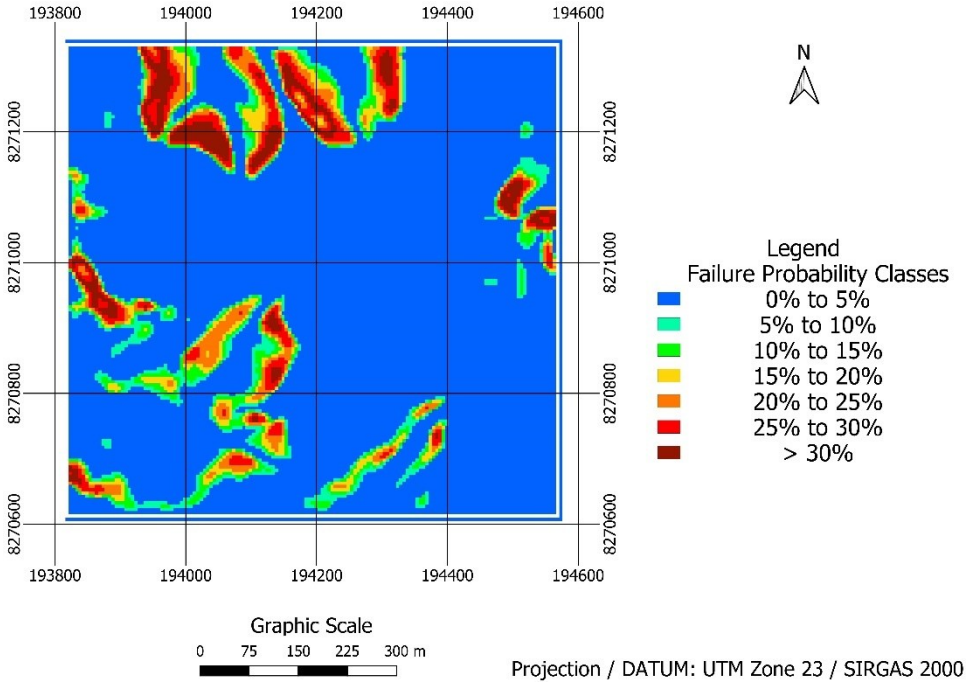

Figure 8 – Monte Carlo Probability of Failure Map ($1x10^7$ simulations).
Source: Authors (2024).

Furthermore, the maximal probability of failure values were calculated for each scenario, as depicted in Table 2.

Table 2 – Maximum probability of failure values.

Number of simulations	**Probabilistic method**	
	Monte Carlo	**FOSM**
10.000	0.3252	0.287741
50.000	0.32653	
100.000	0.32544	
1.000.000	0.32599	
10.000.000	0.32578	

Source: Authors (2024).

Taking into account the overall layout of the assessed area, an observation surfaced: the Monte Carlo method generally yields higher maximum probability of failure values compared to those deduced by the FOSM method.

Hence, an evaluation was conducted to discern the disparity between the probability of failure outcomes acquired from the Monte Carlo method employing $1x10^7$ simulations and those garnered through the FOSM method. This assessment led to the production of the map depicted in Figure 9.

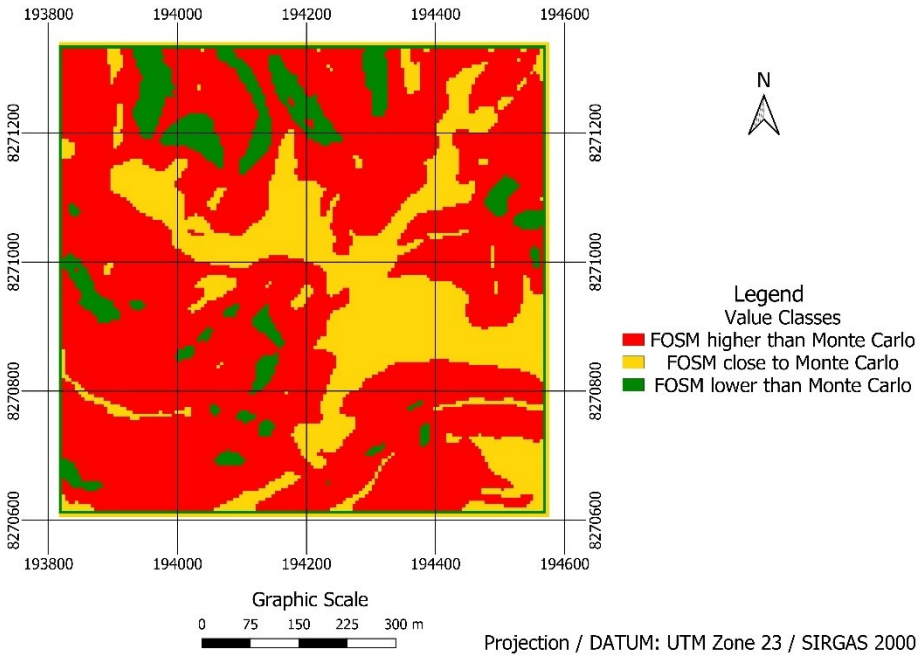

Figure 9 – Values corresponding to the discrepancies between the probabilities of failure obtained from Monte Carlo simulations ($1x10^7$) and the FOSM method.
Source: Authors (2024).

An observation unveils a discernible trend: positive values manifest in areas with steeper slopes, nearing the maximum values. This indicates that, under such circumstances, the Monte Carlo method exhibits higher values. Conversely, null values tend to manifest in flatter regions, signifying a convergence of both methods toward identical outcomes in such conditions. This phenomenon is visually depicted by the pixel distribution within the grid, as exemplified in Table 3.

Table 3 – Cross-tabulation between the slope matrices and the differences between Monte Carlo and FOSM results, categorized by the number of classified pixels.

Slope	**Difference between Monte Carlo ($1x10^7$ simulations) and FOSM**		
	< 0	**0**	**> 0**
0° - 5°	3	1945	0
5° - 10°	131	2013	0
10° - 15°	2243	891	0
15° - 20°	2846	45	0
20° - 25°	2608	3	0
25° - 30°	2466	0	0
30° - 40°	4247	0	380
> 40°	242	0	1244

Source: Authors (2024).

Upon examining the pixel distribution within the matrix, a notable pattern emerges. In most instances, the FOSM method produces probabilities of failure exceeding those generated by the Monte Carlo method, with the exception of elevated regions where a positive difference is evident. Null values, on the other hand, are confined to areas characterized by slopes below 25°, with a notable predominance of slopes below 10°.

Following a methodology analogous to the previous steps, a comparison was drawn between the slope classes using the Monte Carlo method with $1x10^7$ simulations. This analysis yielded the data outlined in Table 4, revealing a notable prevalence of failure probabilities below 5% across all slope classes. Conversely, probabilities exceeding 5% were observed solely within slope classes surpassing 25°.

Table 4 – Cross-tabulation between the slope matrices and the Monte Carlo Method with 1x10^7 simulations, organized by the number of classified pixels.

Slope	Monte Carlo Probability of Failure (1x10^7 simulations)						
	0% - 5%	**5% - 10%**	**10% - 15%**	**15% - 20%**	**20% - 25%**	**25% - 30%**	**> 30%**
0° - 5°	1948	0	0	0	0	0	0
5° - 10°	2144	0	0	0	0	0	0
10° - 15°	3134	0	0	0	0	0	0
15° - 20°	2891	0	0	0	0	0	0
20° - 25°	2611	0	0	0	0	0	0
25° - 30°	2432	33	1	0	0	0	0
30° - 40°	1633	951	744	611	499	185	4
> 40°	15	16	38	96	203	536	582

Source: Authors (2024).

Analyzing the slope values corresponding to the mesh pixels where the Monte Carlo probabilities of failure exceed those of the FOSM method, a total of 1.624 slope values were identified. These findings yield an average slope value of approximately 43.5°, with the highest and lowest values recorded at 55,9° and 36,5°, respectively.

Subsequently, a specific examination of the pixels displaying the utmost and minimum slope values was conducted, scrutinizing the alteration of the probability of failure with varying numbers of simulations. Two pixels were subjected to scrutiny: the initial one situated at row 21 and column 72, denoting the steepest slope value, and the second one situated at row 12 and column 36, depicting the most modest slope value. These fluctuations are visually represented in Figures 10 and 11.

.

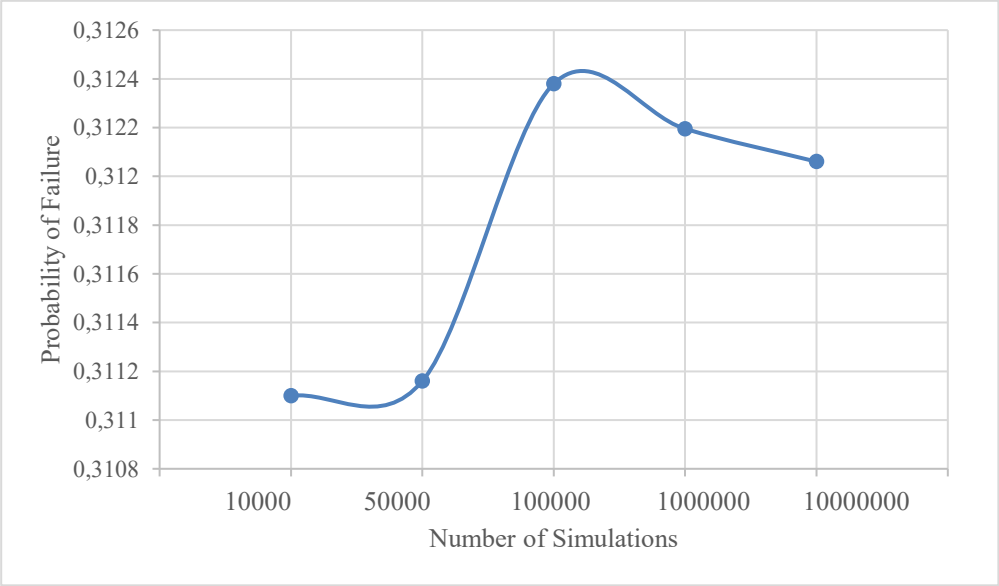

Figure 10 – Variation of the probability of failure in relation to the quantity of Monte Carlo simulations for the pixel associated with the most elevated slope value.
Source: Authors (2024).

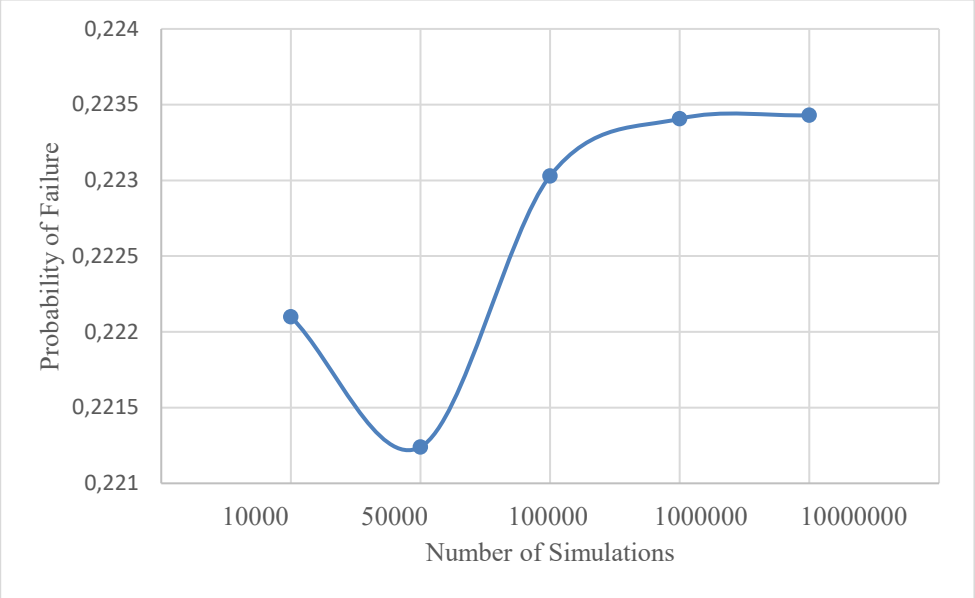

Figure 11 – Variation of the probability of failure with the number of Monte Carlo simulations for the pixel with the lowest slope value.
Source: Authors (2024).

The outcomes from both pixels exhibit lower probability of failure values with fewer simulations. With an increase in the number of simulations, there is a tendency towards an escalation in the probability of failure followed by stabilization. It was observed that for smaller slopes, the probability of failure rises as the number of simulations increases. Conversely, for steeper slopes, the maximum value is attained at 100.000 simulations.

Additionally, deterministic safety factors were computed for the entire study area by utilizing the mean values of cohesion and friction angle in Equation 1. Figure 12 depicts the safety factor map.

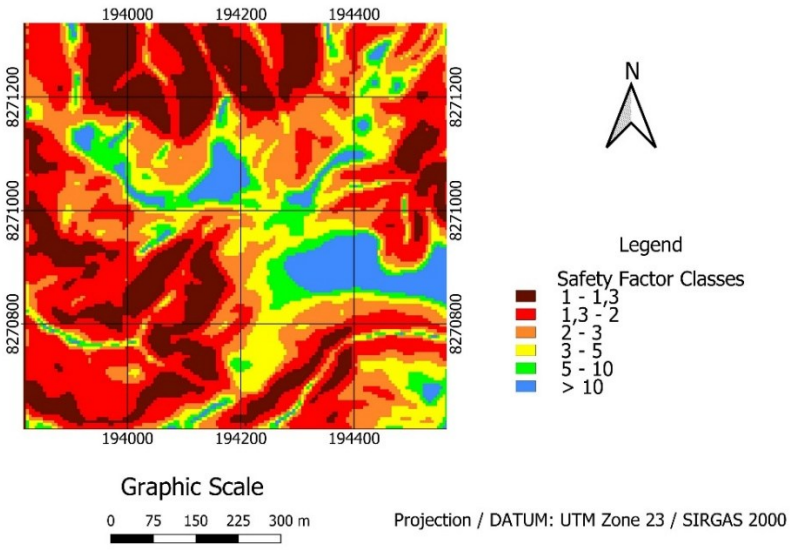

Figure 12 – Deterministic safety factor.
Souce: Authors (2024).

It was observed that the pixel with the highest slope has a safety factor value of 1,1602, while the pixel corresponding to the smallest slope has a safety factor value of 22,6179.

5. Final considerations

Based on the analysis of the failure probabilities, it can be concluded that the Monte Carlo method consistently produces higher maximum values compared to the FOSM method, regardless of the number of simulations used. Nevertheless, both methods exhibit similar spatial distribution patterns for the probability of failure classes. The highest values are concentrated in the northern region of the study area, while the lowest values are clustered in the central region.

Additionally, it was observed that the spatial distributions of failure probabilities resulting from the Monte Carlo method exhibited consistent behavior across all simulation numbers. These distributions displayed a tendency to align with the spatial distribution pattern of the FOSM method as the number of Monte Carlo simulations increased. This convergence in spatial patterns remained even in cases where the Monte Carlo probabilities of failure exceeded those produced by the FOSM method.

Furthermore, it was observed that the Monte Carlo method exhibited a tendency to yield elevated results in regions characterized by steeper slopes. Conversely, in areas with gentler slopes, the method tended to produce values that closely aligned with those obtained from the FOSM method.

Another observed issue is the manner in which the Monte Carlo probability of failure evolves with the progression of simulations, particularly in specific cells. Noteworthy variations associated with the slope were discerned. It was deduced that in areas with milder slopes, there exists a tendency for the probability of failure to rise along with the number of simulations. Conversely, in locations with steeper slopes, the peak value of the probability of failure is attained with a simulation count of 100.000.

Finally, it is worth emphasizing the relevance of the approach proposed in the article for comparing two distinct probabilistic methods: Monte Carlo, which is anticipated to yield "exact" outcomes as the number of simulations approaches infinity, and FOSM, a simplified analytical method. Despite yielding different results, both methods exhibited similar spatial distributions. The diverse probability of failure values obtained from the probabilistic methods are due to the probability distribution type assigned to the cohesion variable as an input. The normal distribution employed in the FOSM method does not constrain cohesion to non-negative values, which shifts the probability distribution of cohesion to the left and results in higher probabilities of failure in comparison to the outcomes obtained by the Monte Carlo method. The Monte Carlo method employs a lognormal distribution (defined for strictly positive values) for cohesion.

References

Azevedo, G. F.; Carvajal, H. E. M.; Souza, N. M. Análise da Ameaça de Deslizamentos pelo Uso de Abordagem Probabilística Aplicada a um Modelo de Estabilidade de Taludes Tridimensional. *Revista Geociências*, v. 37, n. 3, 655-668, 2018.

Beck, A. T. *Confiabilidade e segurança das estruturas*. Rio de Janeiro, Brasil: Elsevier, 2019. 448 p.

Câmara, G.; Souza, R. C. M.; Freitas, U. M.; Garrido, J.; Mitsuo, F. Spring: integrating remote sensing and GIS by object-oriented data modeling. *Journal Computers & Graphics*, v. 20, n. 1, 395-403, 1996.

Catani, F., Segoni, S., Falorni, G. An empirical geomorphology-based approach to the spatial prediction of soil thickness at catchment scale. *Journal Water Resources Research*, v. 46, n. 5, 1-15, 2010.

Chen C. Y.; Lee W. C. Damages to school infrastructure and development to disaster prevention education strategy after Typhoon Morakot in Taiwan. *Disaster Prevention and Management: An International Journal*, v. 21, n. 5, 541- 555, 2004.

Cho, S. E.; Lee, S. R. Evaluation of surficial stability for homogeneous slopes considering rainfall characteristics. *Journal of Geotechnical and Geoenvironmental Engineering*, v. 128, n. 9, 756-763, 2002.

COLLINS, B. D.; ZNIDARCIC, D. Slope stability issues of rainfall induced landslides. In: LISAC, Z.; MARIC, B.; SZAVITS-NOSSAN, A. (Org.). *Geotechnical Hazards*. Rotterdam: Balkema CRC Press, 1998. p. 791-798.

COMPANHIA DE DESENVOLVIMENTO DO PLANALTO CENTRAL – CODEPLAN. *Pesquisa Distrital por Amostra de Domicílios: Sobradinho II*. Organizadores: Jusçanio Umbelino de Souza *et al.* Brasília, DF: CODEPLAN, 2019.

Cordoba, J. P.; Mergili, M.; Aristizábal, E. Probabilistic landslide susceptibility analysis in tropical mountainous terrain using the physically based r.slope.stability model. *NHESS*, v. 20, n. 1, 815-829, 2020.

Cornell, C. C. A probability-based structural code. *Journal of the American Concrete Institute*, v. 66, n. 12, 974-985, 1969.

Frattini, P.; Crosta, G. B.; Fusi, N.; Negro, P. Shallow landslides in pyroclastic soils: a distributed modeling approach for hazard assessment. *Journal Engineering Geology*, v. 73, n. 1, 277-295, 2004.

Furlan, M. C.; Lacruz, M. S. P.; Sausen, T. M. Vulnerabilidade socioeconômica à ocorrência de eventos extremos: proposta metodológica. *In*: Simpósio Brasileiro de Sensoriamento Remoto, 15., 2011, . Anais [...]. Curitiba: INPE. 2011. p. 4540-4546.

Guidicini, G.; Nieble, C. M. *Estabilidade de Taludes Naturais e de Escavação*. São Paulo, Brasil: Edgard Blücher, 1984. 194 p.

Martini, L. C. P.; Uberti, A. A. A.; Scheibe, L. F.; Comin, J. J.; Oliveira, M. A. T. Análise da suscetibilidade a processos erosivos e movimentos de massa: decisão multicriterial suportada em Sistemas de Informações Geográficas. *Revista Geologia USP Série Científica*, v. 6, n. 1, 41-52, 2006.

Montoya, C. A. H.; Assis, A. P. Herramientas para análisis por confiabilidade en geotecnia: La teoria. *Revista Ingenierías* Universidad de Medellín, v. 10, n. 18, 69-78, 2011.

Montgomery, D. R.; Dietrich, W. E. A physically based model for the topographic control on shallow landsliding. *Water Resources Research*, v. 30, n. 4, 1153-1171, 1994.

Nowak, A. S.; Collins, K. R. *Reliability of structures*, 2nd edition. Boca Raton, USA: CRC Press, 2013. 424 p.

Reatto, A.; Martins, E.S.; Farias, M.F.R.; Silva, A.V.; Carvalho JR., O.A.C. *Mapa Pedológico Digital - SIG Atualizado do Distrito Federal Escala 1:100.000 e uma Síntese do Texto Explicativo*. Planaltina, Brasil: Embrapa, 2004, 29 p.

TONUS, B.P.A. *Estabilidade de Taludes*: Avaliação dos métodos de equilíbrio limite aplicados a uma encosta coluvionar e residual da serra do mar paranaense. Curitiba, 2009. 147f. Dissertação (Mestrado em Geotecnia). Programa de Pós-Graduação em Construção Civil, Universidade Federal do Paraná, Curitiba-PR, 2009.

Venancio, A. S.; Pancher A. M.; Cunha C. M. L.; Machado F. B.; Soares Junior A. V. Avaliação da suscetibilidade a movimentos de massa no município de Várzea Paulista (SP) utilizando os sistemas de informação geográfica. *Geociências*, v. 32, n. 1, 81-92, 2013.

Wyllie, D. C.; Mah, C. W. *Rock slope engineering*: Civil and Mining, 4th edition. New York, USA: Spon Press, 2004. 456 p.